PERFORMANCE ANALYSIS OF THE TURBULENCE MODELS FOR A TURBULENT FLOW IN A TRIANGULAR ROD BUNDLE

W. K. In[1*], T. H. Chun[1] and H. K. Myong[2]

A computational fluid dynamics(CFD) analysis has been made for fully developed turbulent flow in a triangular bare rod bundle with a pitch to diameter ratio (P/D) of 1.123. The nonlinear turbulence models predicted the turbulence-driven secondary flow in the triangular subchannel. The nonlinear quadratic k-ε models by Speziale[1] and Myong-Kasagi[2] predicted turbulence structure in the rod bundle fairly well. The nonlinear quadratic and cubic k-ε models by Shih et al.[3] and Craft et al.[4] showed somewhat weaker anisotropic turbulence. The differential Reynolds stress model by Launder et al.[5] appeared to overpredict the turbulence anisotropy in the rod bundle.

Keywords: Rod Bundle, Turbulence, Nonlinear *k-ε* Model, Secondary Flow

1. INTRODUCTION

Most reactor fuel elements generally consist of rod bundles with the coolant flowing axially through the subchannels formed between the rods. The fuel rods are arranged in either square or equilateral triangular pitched arrays. An understanding of the detailed structure of the turbulent flow in a rod bundle, used especially as nuclear fuel elements, is of major interest to the nuclear power industry for their safe and reliable operation.

This paper presents a computational fluid dynamics(CFD) analysis of the turbulent flows in a triangular bare rod bundle by using several nonlinear $k-\varepsilon$ models and a Reynolds stress model(RSM).

2. NONLINEAR TURBULENCE MODEL

In order to improve the weakness of the isotropic eddy viscosity assumption used in the standard $k-\varepsilon$ model, the nonlinear quadratic or cubic relationships for the Reynolds stresses were proposed as follows:

$$\begin{aligned}\rho\overline{u'_i u'_j} &= -\mu_t S_{ij} + \frac{2}{3}\rho k\delta_{ij} + C_1\mu_t\frac{k}{\varepsilon}\\ &\left(S_{ik}S_{kj} - \frac{1}{3}S_{kl}S_{kl}\delta_{ij}\right) + C_2\mu_t\frac{k}{\varepsilon}(\Omega_{ik}S_{kj} + \Omega_{jk}S_{ki})\\ &+ C_3\mu_t\frac{k}{\varepsilon}\left(\Omega_{ik}\Omega_{jk} - \frac{1}{3}\Omega_{lk}\Omega_{lk}\delta_{ij}\right)\\ &+ C_4\mu_t\frac{k^2}{\varepsilon^2}\left(S_{ki}\Omega_{lj} + S_{kj}\Omega_{li}\right)S_{kl} + C_5\mu_t\frac{k^2}{\varepsilon^2}\\ &\left(\Omega_{il}\Omega_{lm} + S_{il}\Omega_{lm}\Omega_{mj} - \frac{2}{3}S_{lm}\Omega_{mn}\Omega_{nl}\delta_{ij}\right) +\\ &C_6\mu_t\frac{k^2}{\varepsilon^2}S_{ij}S_{kl}S_{kl} + C_7\mu_t\frac{k^2}{\varepsilon^2}S_{ij}\Omega_{kl}S_{kl}\end{aligned} \quad (1)$$

where

$$S_{ij} = \left(\frac{\partial U_i}{\partial x_j} + \frac{\partial U_j}{\partial x_i}\right), \Omega_{ij} = \left(\frac{\partial U_i}{\partial x_j} - \frac{\partial U_j}{\partial x_i}\right) - \varepsilon_{ijk}\Omega_k \quad (2)$$

The values of the four empirical coefficients in the quadratic relationship are provided in the references.[1-3] The coefficients for the cubic model by Craft et al.[4] are given as

$$C_\mu = \frac{0.3}{1+0.35(\max(S,\Omega))^{1.5}} \times\left(1-\exp\left[\frac{-0.36}{\exp(-0.75\max(S,\Omega)}\right]\right) \quad (3)$$

Received: June 10, 2004, Accepted: January 19, 2005.
1 Korea Atomic Energy Research Institite
2 Kookmin University
* Corresponding author. E-mail: wkin@kaeri.re.kr

$$C_1 = -0.1, C_2 = 0.1, C_3 = 0.26,$$
$$C_4 = -10C_\mu^2, C_5 = 0, C_6 = -5C_\mu^2, C_7 = 5C_\mu^2$$

Here, S and Ω are the non-dimensional strain rate and vorticity, respectively.

A more complex version of the RANS turbulence model is the differential Reynolds stress model (RSM). It is based on exact transport equations for the individual Reynolds stresses derived from the Navier-Stokes equations. The exact differential equations describe the behavior of the Reynolds-stress tensor τ_{ij} and the dissipation rate ε for an incompressible fluid. The pressure-strain correlation in the RSM uses the Rotta model for a slow pressure strain and the well-known LRR model for a rapid pressure strain.

3. NUMERICAL METHOD

The present analysis simulated the experimental study of the axial turbulent flow in a triangular rod bundle by Carajilescov and Todreas.[6] Only the 1/6 triangular subchannel of the bare rod bundle was modeled by using a flow symmetry to reduce the size of the computational model. Fig. 1 illustrates the triangular rod bundle and the computational grid. The ratio of the pitch to rod diameter(P/D) is 1.123.

The optimal grid is 30x30 in the radial and azimuthal directions, respectively. Since this study simulates the fully developed flow, only two grid cells were used in the main flow direction. The grid size in the nondimensional wall unit(y^+) was calculated to be 15-20, which is the closest distance from the rod surface. The conventional wall functions using a universal law of the wall were applied to specify the turbulence in the near-wall region. The calculations were performed at Reynolds numbers, based on a bulk mean velocity and a hydraulic diameter of 27000.

4. RESULTS AND DISCUSSIONS

Fig. 2 shows the velocity vectors indicating the turbulence-driven secondary flow in the subchannel of the rod bundle. They show the secondary flow from the center of the subchannel to the gap due to an anisotropic turbulence. The maximum secondary velocity was estimated to be 0.8%(Speziale),

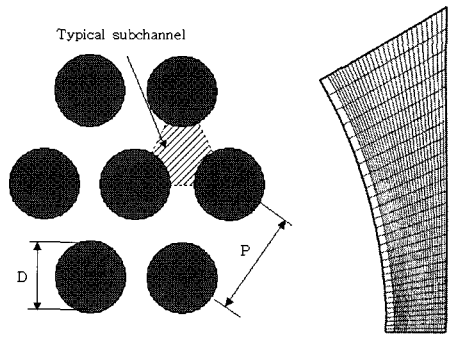

Fig. 1 Layout of a triangular rod bundle and a grid

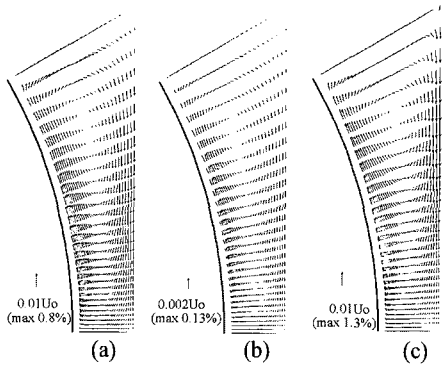

Fig. 2 Turbulence-driven secondary flow: (a) Speziale, (b) Cubic (c) LRR

0.6%(Myong-Kasagi), 0.1%(Shih et al.), 0.13% (Cubic) and 1.3%(LRR) of the bulk mean velocity(Uo), respectively. An experiment[6] has reported that the secondary flows were less than 0.67 percent of the bulk mean velocity. The nonlinear quadratic $k-\varepsilon$ models by Speziale and Myong-Kasagi are judged to predict the secondary velocity reasonably well.

Fig. 3 compares the contour plots for the normalized axial velocity. The axial velocity predicted by the cubic nonlinear $k-\varepsilon$ model appears to decrease more rapidly from the center of the subchannel to the gap region. The Speziale and Myong-Kasagi models show a more accurate velocity distribution but still a lower velocity in the gap region. The RSM by LRR predicted the velocity in the gap region well but a lower value in the center of the subchannel.

Fig. 4 compares the distributions of the turbulent kinetic energy showing a local peak in between the center of the subchannel and the gap. The standard

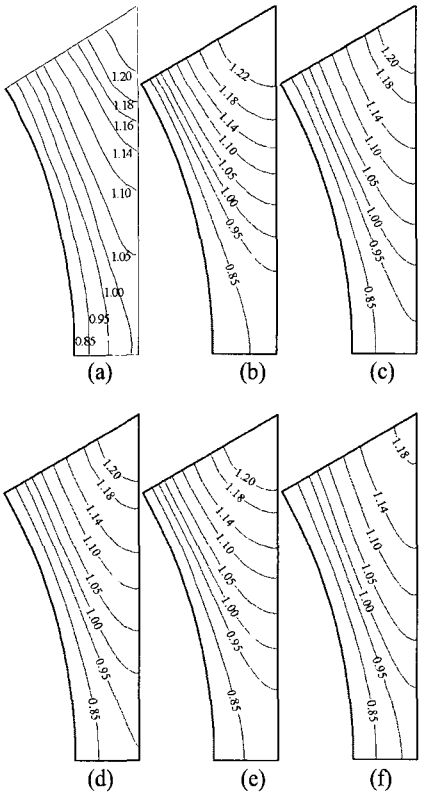

Fig. 3 Distributions of axial velocity (U/Uo):
(a) Experiment, (b) Standard, (c) Speziale,
(d) Myong-Kasagi, (e) Cubic, (f) LRR

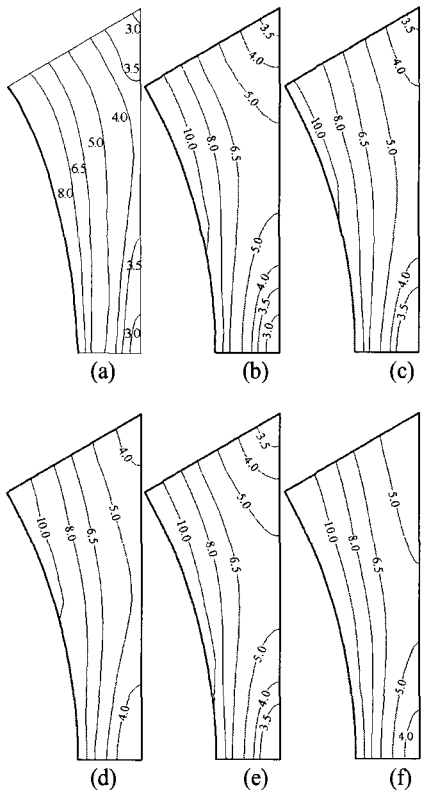

Fig. 4 Distributions of turbulent kinetic energy $(k/Uo^3 \times 10^3)$:
(a) Experiment, (b) Standard, (c) Speziale,
(d) Myong-Kasagi, (e) Cubic, (f) LRR

and cubic $k-\varepsilon$ models showed similar predictions which are somewhat higher than the measurement. The nonlinear model by Shih et al. also showed a distribution similar to the cubic one. The predictions by the Speziale and Myong-Kasagi models agree with the experiment reasonably well. The LRR model shows a higher turbulent kinetic energy and a small variation between the center of the subchannel and the gap.

Fig. 5 shows a comparison of the wall shear stress distribution along the rod surface. It shows an increase from the gap $(\theta = 0)$ to the diagonal $(\theta = 30)$. The nonlinear Shih et al. model and the cubic $k-\varepsilon$ model indicate almost the same results which are slightly better predictions than the standard $k-\varepsilon$. The Speziale and Myong-Kasagi models resulted in predictions showing a peak at $\theta = 25$ and a rapid decrease near the diagonal. The LRR Reynolds stress model predicts the peak at $\theta = 20$. The peak to peak variation of the wall shear

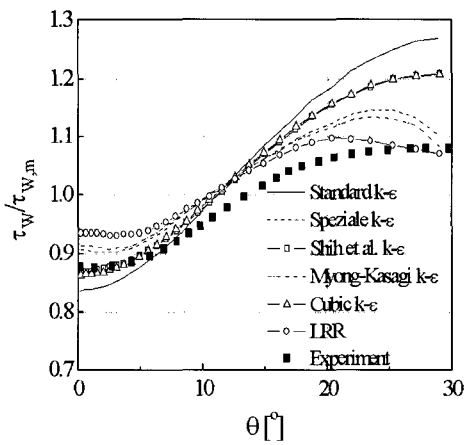

Fig. 5 Wall shear stress distribution along the rod

stress is estimated to be 43%(Standard), 34%(Shih et al. and Cubic), 25%(Speziale and Myong-Kasagi), 17%(RSM) and 20%(Experiment) of the mean value, respectively.

5. CONCLUSION

A CFD analysis has been performed to compare the predictions of the nonlinear turbulence models for an axial turbulent flow in a triangular rod bundle and the following conclusions can be made.

(1) Nonlinear turbulence models predicted the secondary flow in the subchannel of the rod bundle well but showed a large difference in the magnitude of the secondary velocity.

(2) The quadratic .models proposed by Speziale and Myong-Kasagi predict the turbulent flow characteristics in the rod bundle fairly well. The Reynolds stress model by Launder et al. overpredicts the turbulence-driven secondary flow and the turbulent kinetic energy.

(3) The nonlinear turbulence models need to be evaluated further for their prediction performance of a detailed turbulence structure in a rod bundle.

ACKNOWLEDGMENT

The authors express their appreciation to the Ministry of Science and Technology of Korea for financial support.

REFERENCES

[1] Speziale, C.G., 1987, "On Non-linear k-l and $k-\varepsilon$ Models of Turbulence," *J. Fluid Mech.*, Vol.178, pp.459-475.

[2] Myong, H.K. and Kasagi, N., 1990, "Prediction of Anisotropy of the Near Wall Turbulence with an Anisotropic Low-Reynolds-number $k-\varepsilon$ Turbulence Model," *J. Fluids. Eng.*, Vol.112, pp.521-524.

[3] Shih, T.H., Zhu, J. and Lumley, J.L., 1993, "A Realizable Reynolds Stress Algebraic Equation Model," *NASA tech. memo. 105993.*

[4] Craft, T.J., Launder, B.E. and Sugar, K., 1996, "Development and Application of a Cubic Eddy-viscosity Model of Turbulence," *Int. J. Heat and Fluid Flow*, Vol.17, No.2, pp.108-115.

[5] Launder, B.E., Reece, G.J. and Rodi, W., 1974, "Progress in the Development of a Reynolds Stress Turbulence Model," *J. Fluid Mech.*, Vol.68, pp.269-289.

[6] Carajilescov, P. and Todreas, N.E., 1976, "Experimental and Analytical Study of Axial Turbulent Flows in an Interior Subchannel of a Bare Rod Bundle," *J. Heat Transfer*, pp.262-268.